19

Kinematic Analysis of 3-UCR Parallel Robot Leg

Cheng Gang and Ge Shi-rong
College of Mechanical and Electrical Engineering Xuzhou
China University of Mining and Technology
China

1. Introduction

Mine rescue robot was developed to enter mines during emergencies, such as underground explosion, roof fall or water inundation, to locate possible escape routes for those trapped inside and determine whether it is safe for human to enter or not. Comparing with wheeled robots (Baker et al., 2004) and tracked robots (Tanaka et al., 2005; Wang et al., 2007), legged robots are flexible and effective to move on uneven surfaces and natural environments because of its adaptability to the geometry of the terrain and in principle support on very steep surfaces. Though thought as the promising systems, it is always challenging and complex to achieve robust locomotion of legged robots.

Most of the recent prototypes of legged robots, including Lauron III (Gabmann et al., 2005), RHex (Koditschek et al., 2004) and SILO4 (Santos et al., 2005), adopted the serial leg manipulator. Due to better system rigidity, rapid motion velocity, high nominal load to weight ratio and flexible end position-stance, the parallel manipulators are feasible to be the leg manipulators of mine rescue robots. But it is well known that the close chain often leads to difficulty in its mechanical design. Since Clavel and his Delta structures (Clavel, 1988) in the late 80's have reached extremely high performances, lower-mobility parallel manipulators have been under intensive study for over many years. Lower-mobility parallel manipulators have simpler mechanical structure, simpler control system, high speed performance, low manufacturing and operations cost (Kim, 2001). Therefore, they have been applied in some fields, including telescope applications (Carretero et al., 2000), flight simulation (Pouliot et al., 1996) and beam aiming applications (Dunlop & Jones, 1997). Among lower-mobility parallel manipulators, special attention has been paid to optimization and innovation of 3 degree-of-freedom (DOF) parallel manipulators. Some 3-DOF translational and spherical parallel manipulators were proposed respectively.

The topological structure of 3-UCR symmetrical parallel robot leg is described in Fig. 1(a). The parallel manipulator consists of a fixed base, a moving platform and three limbs with identical structure. In Fig. 1(a), O_O-$X_OY_OZ_O$ is the static coordinate system attached to the base, while $O_{O'}$-$X_{O'}Y_{O'}Z_{O'}$ is the moving coordinate system attached to the moving platform. The lengths of the equilateral triangle lines in the moving platform and the base, such as $L_{A'B'}$ and L_{AB}, are denoted as L_m and L_B, respectively. Each limb connects the moving

platform to the base by a revolute joint (R) followed by cylindrical joint (C) and universal joint (U) in sequence. The lengths of limbs are given as $L_{II'}$ where I can be substituted by A, B, C.

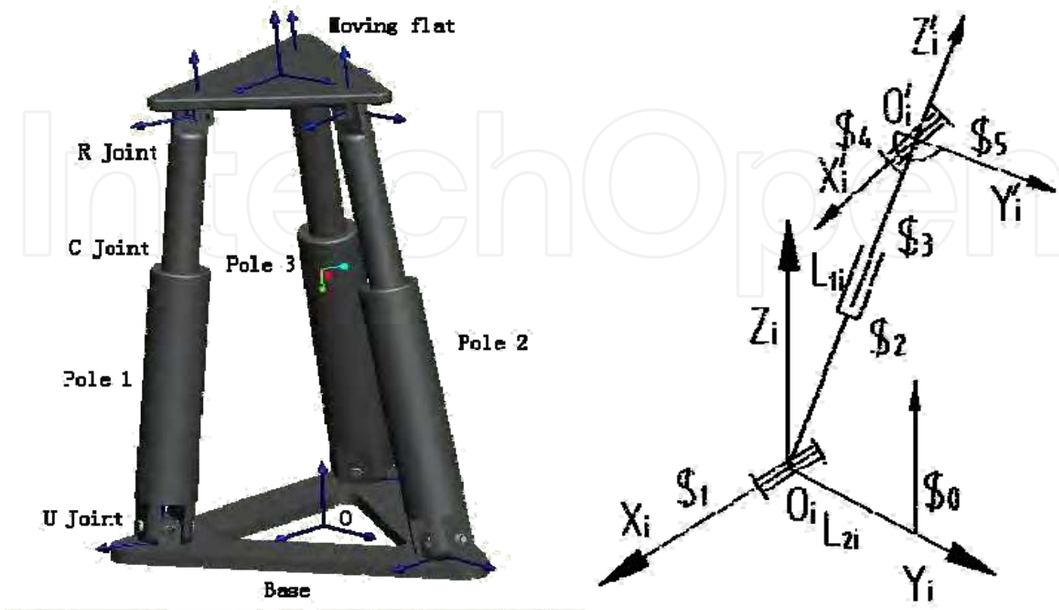

Fig. 1. 3-UCR spatial parallel manipulator: (a) 3-UCR parallel manipulator, (b) UCR topological limb

As shown in Fig. 1(a), the number of links is n=8 for 1 platform, 3 cylinders, 3 piston-rods, and 1 base; the number of joints is 9 for 3 revolute joints, 3 cylindrical joints, and 3 universal joints. Based on a revised Kutzbach-Grübler equation, the DOF of 3-UCR parallel robot leg is 3. Therefore, any screw of the manipulator consisted of three linearly independent principal screws and it is known as third-order screw system.

2. Instantaneous Kinematic Characteristics of 3-UCR Parallel Robot Leg

The performance of parallel robot leg largely depends on the characteristics of the end-effector, including the DOF number, workspace, singularity and dynamic performance, decided by the instantaneous kinematics. Because of the kinematic coupling of parallel robot leg caused by the interaction of limbs, it is complicated to describe the instantaneous kinematics of parallel robot leg. The reciprocal screw theory was introduced by Fang and Alon and the spatial screw restrictions were used to analyze the kinematic characteristics of moving platform (Fang & Tsai, 2004; Alon & Moshe, 2006). Sokolov made the similar study on the basis of differential geometrical method and he further developed the singularities of moving platform (Sokolov & Xirouchakis, 2006). For the purpose of the instantaneous kinematic analysis of 3-UCR parallel robot leg with 2R1T DOF, the principal screw theory in reciprocal screw theory can be proposed to analyze the robot leg. By contrast with the first-order influence coefficient matrix between base and moving platform, the principal screw model can be established. So the spatial screw restrictions and the corresponding kinematics of moving platform can be also obtained.

2.1 Principal Screw Theory

Screw theory is important to analyze the kinematic characteristics of manipulators. The principal screws intersect perpendicularly each other in screw system, and the number of principal screws equals to the order of screw system. The principal screws describe the instantaneous independent motion of rigid body, and any screw in screw system is the linear combination of principal screws. Therefore, the principal screws are an important tool in the analysis of kinematic characteristics. In order to further understand the kinematic nature and all possible motions of the manipulators at any given instant, the principal screws of the manipulators should be identified from screw system. Compared with the principal screws in second-order screw system, the solving process of principal screws in third-order screw system is more complicated and there are three principal screw pitches h_1, h_2 and h_3. All screw pitch values exist in the scale between two extreme values denoted as h_1 and h_3. Ball deduced the principal screws of third-order system by means of mapping geometry method (Ball, 1900) and Fang analyzed for the same purpose based on conic section degenerating theory (Fang & Huang, 1998).

The study (Hunt, 1978) indicated that the quadric surface would degenerate into principal screw axis 1or 3 when $h=h_1$ or $h=h_3$. The quadric surface would degenerate into a pair of intersecting planes and the corresponding intersecting line is principal screw axis 2 when $h=h_2$. The middle symmetry axis in hyperboloid of one sheet is regarded as principal screw axis 1, and the semi-major axis of middle ellipse is principal screw axis 2 when $h_1>h>h_2$. The mid-symmetry axis in hyperboloid of one sheet is principal screw axis 3, and the semi-major axis of middle ellipse in the plane decided by axis 1 and axis 2 is still axis 2 when $h_2>h>h_3$. The second equation would degenerate if any pitch value in the system equals to any of h_1, h_2 and h_3. For example, the planar quadratic equation would degenerate into two virtual lines crossing vertically at one point when $h=h_1$ or $h=h_3$, and the equation would degenerate into two solid lines when $h=h_2$.

Based on the screw theory (Hunt, 1978), a screw can be written as

$$\$ = \left(S, S_0 + hS\right), \tag{1}$$

where S, S_0 denote the direction and position of a line in space respectively and h is the pitch of the screw. $h=0$ and $h=\infty$ correspond to pure rotation and pure translation of a rigid body, and the screw will have the form (S, S_0) and (0, hS) respectively.

2.2 Principal Screw Model

From the theory as above mentioned, the screw pitch of rotation joint and translation joint respectively is 0 and ∞. For the purpose of analyzing DOF and kinematics characteristics of 3-UCR parallel robot leg, the revolute and cylindrical characteristics of moving parts should be obtained. Therefore, it is necessary to put emphasis on the analysis of principal screw pitch.

In order to solve the principal screw pitch, the first-order influence coefficient matrix G and G' need to be analyzed firstly. The first-order influence coefficient matrix G_i^0 (i=1, 2, 3) of limbs can be deduced by means of imaginary mechanism principle as

$$\left[G_i^0\right] = \left[A_i^0\right]\left[\$_0^{(i)} \quad \$_1^{(i)} \quad \$_2^{(i)} \quad \$_3^{(i)} \quad \$_4^{(i)} \quad \$_5^{(i)}\right], \tag{2}$$

where A_i^0 is the transform matrix between the limb coordinate system and the static coordinate system. So the equation about the angular velocity ω of the end-effector in moving platform, the linear velocity v_p of the chosen reference point and the input velocity vector $\dot{\xi}^{(i)}$ of every limb can be shown as

$$\begin{bmatrix}\omega & v_P\end{bmatrix}^T = \begin{bmatrix}G_i^0\end{bmatrix}\begin{bmatrix}\dot{\xi}_0^{(i)} & \dot{\xi}_1^{(i)} & \dot{\xi}_2^{(i)} & \dot{\xi}_3^{(i)} & \dot{\xi}_4^{(i)} & \dot{\xi}_5^{(i)}\end{bmatrix}. \tag{3}$$

If the matrix $\begin{bmatrix}G_i^0\end{bmatrix}$ is non-singular, there would be $\begin{bmatrix}G_0^i\end{bmatrix} = \begin{bmatrix}G_i^0\end{bmatrix}^{-1}$. If the velocities of cylindrical joint 1 and 3 can be chosen as the input velocities in third-order screw system, taking and combining the first row and third row corresponding to $\xi_0^{(i)}$ and $\xi_2^{(i)}$ from the matrix $\begin{bmatrix}G_0^i\end{bmatrix}$ of every limbs in Eq. (3) could get the following equation as

$$\begin{bmatrix}G_H^q\end{bmatrix} = \begin{bmatrix}\begin{bmatrix}G_0^1\end{bmatrix}_3 & \begin{bmatrix}G_0^2\end{bmatrix}_3 & \begin{bmatrix}G_0^3\end{bmatrix}_3 & \begin{bmatrix}G_0^1\end{bmatrix}_1 & \begin{bmatrix}G_0^2\end{bmatrix}_1 & \begin{bmatrix}G_0^3\end{bmatrix}_1\end{bmatrix}^T \in R^{6\times 6}. \tag{4}$$

The manipulators with different DOF need different number of input parameters, except for redundant driving, so the forms of first-order influence matrix G and G' are decided by the number of DOF. Since 3-UCR manipulator has three DOF, it is necessary to have three inputs. Therefore, the corresponding relation of inputs and outputs can be established as

$$\begin{bmatrix}\omega & v_P\end{bmatrix}^T = \begin{bmatrix}G_L^H\end{bmatrix}\begin{bmatrix}\dot{L}_1 & \dot{L}_2 & \dot{L}_3\end{bmatrix} = \begin{bmatrix}G' & G\end{bmatrix}\begin{bmatrix}\dot{L}_1 & \dot{L}_2 & \dot{L}_3\end{bmatrix}, \tag{5}$$

where $\dot{L}_1$, $\dot{L}_2$, $\dot{L}_3$ are the known input velocities of limbs and G_L^H formed by taking the first three columns of $\begin{bmatrix}G_H^q\end{bmatrix}^{-1}$ is a 6×3 matrix.

Fang analyzed the screw characteristics of instantaneous kinematics of robot, and the pitch and the axis of screw can be solved as

$$h = \frac{\{\mu \quad \sigma \quad 1\}^T [G']^T [G] \{\mu \quad \sigma \quad 1\}}{\{\mu \quad \sigma \quad 1\}^T [G']^T [G'] \{\mu \quad \sigma \quad 1\}}, \tag{6}$$

$$[r][G']\{\mu \quad \sigma \quad 1\}] = ([G] - h[G'])\{\mu \quad \sigma \quad 1\}, \tag{7}$$

where $(\mu \quad \sigma) = (\dot{L}_1/\dot{L}_3 \quad \dot{L}_2/\dot{L}_3)$.

It is obviously that any pair of variables (μ, σ) corresponds to a screw in space. Therefore, the screw in third-order system can be represented by using any point (μ, σ). Eliminating (x, y, z) from Eq. (6), we obtain

$$a_{11}\mu^2 + 2a_{12}\mu\sigma + a_{22}\sigma^2 + 2a_{13}\mu + 2a_{23}\sigma + a_{33} = 0, \tag{8}$$

where 3×3 matrix a_{ij} (i, j=1, 2, 3) is the function about screw pitch of moving platform and elements of matrix [G] and [G'].

If the quadric curve expressed by Eq. (8) degenerates, that is σ becomes the linear function of μ, the following condition must be satisfied,

$$D = \begin{vmatrix} a_{11} & a_{12} & a_{13} \\ a_{21} & a_{22} & a_{23} \\ a_{31} & a_{32} & a_{33} \end{vmatrix} = 0 . \tag{9}$$

Expending Eq. (9), we obtain

$$c_1 h^3 + c_2 h^2 + c_3 h + c_4 = 0 , \tag{10}$$

where the coefficients c_i (i=1, 2, 3, 4) are formed by the elements in matrix [G] and [G']. Three possible roots corresponding to the pitches of three principal screws can be obtained by solving Eq. (10), and the instantaneous characteristics of the manipulator can be gotten by analyzing them.

2.3 Screw Analysis of 3-UCR Parallel Robot Leg

In order to solve first-order influence coefficient matrixes, the limb screw system should be constructed as shown in Fig. 1(b) by means of imaginary mechanism principal firstly. An imaginary link and an imaginary revolute pair denoted by a screw with zero pitch are added to every limb. Moreover, there are five unit-DOF kinematic pairs in every limb of 3-UCR parallel robot leg. So every limb of this manipulator has six unit pairs. For the purpose of keeping equivalent kinematic effect between the imaginary manipulator and the real one, let the velocity amplitude of the imaginary unit screw $\$_0$ of every limb be zero, and $\$_0$ is linearly independent with the other five real screws of the primary limb. Therefore, the plücker coordinate of the imaginary screw $\$_0$ in the static coordinate system is

$$\$_0 = (0 \quad 0 \quad 1 \quad l_2 \quad 0 \quad 0), \tag{11}$$

where l_2 is the length from the origin to the centers of three imaginary pairs which is shown in Fig. 1(b). And the plücker coordinates of three original limbs in base system are

$$\left.\begin{aligned} \$_1 &= (0 \quad 1 \quad 0 \quad 0 \quad 0 \quad 0), \\ \$_2 &= (0 \quad 0 \quad 0 \quad -\sin(\alpha_i) \quad 0 \quad \cos(\alpha_i)), \\ \$_3 &= (-\sin(\alpha_i) \quad 0 \quad \cos(\alpha_i) \quad 0 \quad 0 \quad 0), \\ \$_4 &= (0 \quad 1 \quad 0 \quad l_{1i}\cos(\alpha_i) \quad 0 \quad l_{1i}\sin(\alpha_i)), \\ \$_5 &= (\cos(\alpha_i) \quad 0 \quad \sin(\alpha_i) \quad 0 \quad -l_{1i} \quad 0), \end{aligned}\right\} \tag{12}$$

where l_{1i} is the instantaneous length of every limb and α_i is the angel between limb l_i and Z_i in the limb coordinate system, $\alpha_i = \arcsin((r - r')/l_i)$. The first-order influence matrix G_i^0 of every limb can be obtained by Eq. (11) and Eq. (12). By selecting the imaginary pair and

the prismatic motion in cylindrical joint as the initiative inputs, the influent matrix G_H^q can be obtained as

$$G_H^q = \begin{bmatrix} 0 & -c\alpha_1 & 0 & -s\alpha_1 & 0 & c\alpha_1 \\ \frac{\sqrt{3}rc\alpha_2}{2} & \frac{1}{2rc\alpha_2} & 0 & \frac{s\alpha_2}{2} & \frac{-\sqrt{3}s\alpha_2}{2} & c\alpha_2 \\ \frac{\sqrt{3}rc\alpha_3}{2} & \frac{1}{2rc\alpha_3} & 0 & \frac{s\alpha_3}{2} & \frac{\sqrt{3}s\alpha_3}{2} & c\alpha_3 \\ \frac{l_{11}c\alpha_1}{l_2+l_{11}s\alpha_1} & 0 & \frac{r+l_{11}s\alpha_1}{l_2+l_{11}s\alpha_1} & 0 & \frac{1}{(l_2+l_{11}s\alpha_1)} & 0 \\ \frac{-l_{12}c\alpha_2}{2(l_2+l_{12}s\alpha_2)} & \frac{\sqrt{3}l_{12}c\alpha_2}{2(l_2+l_{12}s\alpha_2)} & \frac{r+l_{12}s\alpha_2}{l_2+l_{12}s\alpha_2} & \frac{-\sqrt{3}}{2(l_2+l_{12}s\alpha_2)} & \frac{-1}{2(l_2+l_{12}s\alpha_2)} & 0 \\ \frac{-l_{13}c\alpha_3}{2(l_2+l_{13}s\alpha_3)} & \frac{-\sqrt{3}l_{13}c\alpha_3}{2(l_2+l_{13}s\alpha_3)} & \frac{r+l_{13}s\alpha_3}{l_2+l_{13}s\alpha_3} & \frac{\sqrt{3}}{2(l_2+l_{13}s\alpha_3)} & \frac{-1}{2(l_2+l_{13}s\alpha_3)} & 0 \end{bmatrix}. \quad (13)$$

The first-order influence coefficient matrixes G and G' of 3-UCR parallel robot leg can be solved by the above principal screw model, and the pitches of the general screw can be gotten by Eq. (6) and Eq. (10). Analyzing the pitches shows that 3-UCR parallel robot leg with different position and orientation has only 3 DOF including 2R1T. In the following part, the principal screw when the base is parallel to the moving platform, as an example of numerical simulation, would be analyzed.

2.4 Analysis of principal screw when the base is parallel to the moving platform

According to the topological structure of UCR limb, the parameters need to be taken in this configuration. They are l_{1i}=180mm, l_2=35mm, r=45mm, and r'=35mm. By substituting those parameters into the above principal screw model, we obtain the influent matrix G_H^q as

$$G_H^q = \begin{bmatrix} 0 & -49.938 & 0 & -4.9979\times10^{-2} & 0 & 9.9875\times10^{-1} \\ 43.248 & 24.969 & -7.4742\times10^{-17} & 2.4989\times10^{-2} & -4.3283\times10^{-2} & 9.9875\times10^{-1} \\ -43.248 & 24.969 & 7.4742\times10^{-17} & 2.4989\times10^{-2} & 4.3283\times10^{-2} & 9.9875\times10^{-1} \\ 3.9953 & 0 & 1.2 & 0 & 2.0002\times10^{-2} & 0 \\ -1.9976 & 3.46 & 1.2 & -1.7322\times10^{-2} & -0.01 & -6.9389\times10^{-18} \\ -1.9976 & -3.46 & 1.2 & 1.7322\times10^{-2} & -0.01 & 6.9389\times10^{-18} \end{bmatrix}. \quad (14)$$

By analyzing the previous equation, the first-order influence coefficient matrixes G and G' are written as

$$G = \begin{bmatrix} -2.2224 & 1.1112 & 1.1112 \\ 4.4409\times10^{-16} & -1.9246 & 1.9246 \\ 3.3375\times10^{-1} & 3.3375\times10^{-1} & 3.3375\times10^{-1} \end{bmatrix}, \quad (15)$$

$$G' = \begin{bmatrix} -1.7347\times10^{-18} & 9.635\times10^{-3} & -9.635\times10^{-3} \\ -1.1126\times10^{-2} & 5.5629\times10^{-3} & 5.5629\times10^{-3} \\ 3.7565\times10^{-18} & -2.3217\times10^{-16} & 2.2927\times10^{-16} \end{bmatrix}. \quad (16)$$

Substituting Eq. (14) and Eq. (15) into Eq. (6) gets the following equation as

$$9.0939\times10^{-44}h^3 + 6.097\times10^{-26}h^2 + 1.8077\times10^{-36}h - 1.1126\times10^{-49} = 0. \quad (17)$$

By solving Eq. (16), the pitches of the instantaneous 3-UCR parallel robot leg are obtained as

$$h = \begin{bmatrix} -6.7045\times10^{17} & -2.971\times10^{-9} & 6.1421\times10^{-12} \end{bmatrix}. \quad (18)$$

From the Eq. (18), it is shown that two possible roots of h are close to zero and one possible root of h can be seen as infinite in spite of any inputs. Based on the definition of screw theory, we can see that the screw is pure rotation when the pitch is zero and pure translation when the pitch is close to infinite. Therefore, the 3-UCR parallel robot leg has two instantaneous rotations and one instantaneous translation when the base is parallel to the moving platform.

3. Inverse Kinematic Analysis of 3-UCR Parallel Robot Leg

For better motion control, it is essential to analyze the kinematics of the parallel robot leg. Kim and Park considerably simplified the kinematic algorithm of 3-RS parallel manipulator based on Sylvester's elimination method (Kim & Park, 2001). Kindermann and Cruse proposed the mean of multiple computations to solve the kinematics of manipulators of nearly arbitrary configuration and validated the method by the calculation of a hexapod walking system (Kindermann & Cruse, 2002). Sokolov introduced subtly some novel geometrical parameters and established the inverse kinematic model about a 3-RPS parallel manipulator (Sokolov & Xirouchakis, 2005). Through the double semi-ellipses approximate distribution model, Wang obtained the corrected inverse kinematic solution of the variable geometry parallel manipulator (Wang & Yang, 2005). It is necessary to choose the descriptions of the attitude motion of rigid bodies including direction-cosine, Euler angles, quaternion and Rodrigues parameters. But direction-cosine method needs nine parameters and six constraint equations and it is difficult to be solved. Quaternion method has four parameters which is more than the least number of parameters required to describe the orientation of a rotating rigid body that is three. Though described by three parameters, Euler angle method has singularities. Such this case is Rodirgues parameters can be used. Moreover, Rodrigues parameters stand for trigonometric functions in the kinematic model and improve the ability of real-time control. But when calculating by Rodirgues parameters, eigenaxis rotations greater than 180° cannot be allowed because of the corresponding singularities. The kinematic characteristics of the parallel robot leg decide that its motions are within the range of angle limits. So Rodrigues parameter method is adopted to describe the parallel robot leg.

3.1 RODRIGUES PARAMETERS

In 1840, Rodrigues published a paper on the transformation groups, and Rodrigues parameters that integrate the direction cosines of a rotation axis with the tangent of half the rotation angle were presented with three quantities. The angles of the rotations appear as half-angles which occurred for the first time in the study of rotations. The half-angles are an essential feature of the parameterization of rotations and are the measure of pure rotation for the most elegant representation of rotations in kinematics (Dai, 2006). The Rodrigues parameters were further taken by Cayley to comprise a skew symmetric matrix which then formed Cayley's formula (Cayley, 1875) for a rotation matrix (Altmann, 1986).

Cayley-Rodrigues parameters can be used to eliminate the constraints associated with the Euler parameters, and further these parameters reduce the number of coordinates that describe the rigid body orientation from four to three. This fact can be established by defining so-called Cayley-Rodrigues parameters as follows:

$$\Phi_i = \lambda_i / \lambda_0 \qquad (i=1, 2, 3), \tag{19}$$

where λ_i (i=0, 1, 2, 3) are defined as the Euler parameters.

The Cayley-Rodrigues parameters λ_i (i=1, 2, 3) are also components of the Gibbes which defined as

$$\Phi_i = \hat{p}_i \tan(\theta/2) \quad (i=1, 2, 3), \tag{20}$$

where $\hat{p}_i$ (i=1, 2, 3) are the components of principal vector of rotation $\hat{p}$ referred to the body axes.

Considering Φ_i (i=1, 2, 3) as the projection of connected coordinates composes the Rodrigues vector denoted as $\mathbf{\Phi}$. So the direction-cosine matrix with Rodrigues parameters can be written as

$$\mathbf{A} = \frac{1}{1+\Phi_1^2+\Phi_2^2+\Phi_3^2} \begin{bmatrix} 1+\Phi_1^2-\Phi_2^2-\Phi_3^2 & 2(\Phi_1\Phi_2-\Phi_3) & 2(\Phi_1\Phi_3+\Phi_2) \\ 2(\Phi_2\Phi_1+\Phi_3) & 1-\Phi_1^2+\Phi_2^2-\Phi_3^2 & 2(\Phi_2\Phi_3-\Phi_1) \\ 2(\Phi_3\Phi_1-\Phi_2) & 2(\Phi_3\Phi_2+\Phi_1) & 1-\Phi_1^2-\Phi_2^2+\Phi_3^2 \end{bmatrix}. \tag{21}$$

3.2 Inverse kinematics of moving platform

As shown in the topological figure of 3-UCR parallel robot leg, $O_0I'O_0'$ is considered as the closed-loop kinematic chain, and the corresponding vector of the chain can be written as

$$\overrightarrow{O_0I'} = \mathbf{A}\overrightarrow{O_0'I'} + \overrightarrow{O_0O_0'}, \tag{22}$$

where O_0I', $O_0'I'$ and O_0O_0' correspond to the coordinates of the vector O_oI', O_o'I' and O_oO_o', respectively.

Due to the geometrical characteristics of the parallel manipulator, the kinematic spaces of limbs are limited in three planes that are defined, respectively, as x=0 in limb AA', $x=-\sqrt{3}y$ in limb BB' and $x=\sqrt{3}y$ in limb CC'. So substituting Eq. (21) into Eq. (22) gives the following equations:

$$\Phi_3 = 0\,, \tag{23}$$

$$x_{O'} = -2L_m\Phi_1\Phi_2 \big/ \sqrt{3}\lambda_0^2\,, \tag{24}$$

$$y_{O'} = L_m\left(\Phi_2^2 - \Phi_1^2\right) \big/ \sqrt{3}\lambda_0^2\,. \tag{25}$$

Suppose that the velocity of origin on the moving coordinate system is denoted as $V_{O'}$ and the corresponding sub-velocities along coordinate axes are denoted as $V_{O'x}$, $V_{O'y}$, and $V_{O'z}$. According to the corresponding differential equations of the above three equations with respect to time, the sub-velocities can be written as

$$V_{O'x} = 2L_m\left(\Phi_2\left(1-\Phi_1^2+\Phi_2^2\right)\dot{\Phi}_1 + \Phi_1\left(1+\Phi_1^2-\Phi_2^2\right)\dot{\Phi}_2\right) \big/ \sqrt{3}\lambda_0^4\,, \tag{26}$$

$$V_{O'y} = 2L_m\left(-\Phi_1\left(1+2\Phi_2^2\right)\dot{\Phi}_1 + \Phi_2\left(1+2\Phi_1^2\right)\dot{\Phi}_2\right) \big/ \sqrt{3}\lambda_0^4\,, \tag{27}$$

$$V_{O'z} = \dot{z}\,, \tag{28}$$

where λ_0^2 equals to $1+\Phi_1^2+\Phi_2^2$ and $\dot{\Phi}_1$, $\dot{\Phi}_2$ represent the change velocities of the corresponding Rodrigues parameters, respectively.

Suppose that the angular velocity of origin on the moving coordinate system is denoted as $\boldsymbol{\omega}_{O'}$. Analyzing the geometrical characteristics of the parallel manipulator with 3-UCR limbs gives the following equation as

$$\mathbf{V}_{I'} = \mathbf{V}_{O'} + \boldsymbol{\omega}_{O'} \times \overline{O'I'}\,, \tag{29}$$

where $\mathbf{V}_{I'}$ (I'=A', B', C') represents the velocity of the connectors on the moving platform relative to the static coordinate system and the vector between O' and I' is denoted as $\overline{O'I'}$. Due to the restrictions of revolute joints on the base, the limb coordinates are located in three planes perpendicular to the axes of revolute joints. The normalization of the three axes can be obtained as $\mathbf{e}_A = \left(-1\ 0\ 0\right)^T$, $\mathbf{e}_B = \left(1/2\ \sqrt{3}/2\ 0\right)^T$ and $\mathbf{e}_C = \left(1/2\ -\sqrt{3}/2\ 0\right)^T$, so one can have

$$\mathbf{V}_{I'}\mathbf{e}_I = 0\,. \tag{30}$$

Analyzing the above equation gives the angular velocities of centroid on the moving platform as follows:

$$\omega_{O'x} = \frac{\left(s_{22}s_{33}-s_{32}s_{23}\right)s_{41} + \left(s_{31}s_{23}-s_{33}s_{21}\right)s_{42} + \left(s_{32}s_{21}-s_{31}s_{22}\right)s_{43}}{s_{12}\left(s_{33}s_{21}-s_{31}s_{23}\right) + s_{13}\left(s_{31}s_{22}-s_{32}s_{21}\right)}\,, \tag{31}$$

$$\omega_{O'y} = \frac{\left(s_{13}s_{32}-s_{12}s_{33}\right)s_{41} - s_{13}s_{31}s_{42} + s_{12}s_{31}s_{43}}{s_{12}\left(s_{33}s_{21}-s_{31}s_{23}\right) + s_{13}\left(s_{31}s_{22}-s_{32}s_{21}\right)}\,, \tag{32}$$

$$\omega_{O'z} = \frac{\left(s_{12}s_{23}-s_{13}s_{22}\right)s_{41} + s_{13}s_{21}s_{42} - s_{21}s_{12}s_{43}}{s_{12}\left(s_{33}s_{21}-s_{31}s_{23}\right) + s_{13}\left(s_{31}s_{22}-s_{32}s_{21}\right)}\,, \tag{33}$$

where the variables in the above three equations can be expressed analytically.

According to the differential forms of sub-velocities of origin on the moving coordinate system with respect to time, the corresponding linear accelerations can be obtained as

$$a_{O'x} = \dot{V}_{O'x}\,, \tag{34}$$

$$a_{O'y} = \dot{V}_{O'y}\,, \tag{35}$$

$$a_{O'z} = \dot{V}_{O'z}\,. \tag{36}$$

Similarly, the differential forms of angular velocities of origin on the moving coordinate system with respect to time give the corresponding angular acceleration as

$$\zeta_{O'x} = \dot{\omega}_{O'x}\,, \tag{37}$$

$$\zeta_{O'y} = \dot{\omega}_{O'y}\,, \tag{38}$$

$$\zeta_{O'z} = \dot{\omega}_{O'z}\,. \tag{39}$$

3.3 Inverse kinematics of limbs

The coordinates of the connectors in the moving platform being reference to the static coordinate system can be obtained by substituting Eq. (23), Eq. (24) and Eq. (25) into Eq. (22). So the lengths of limbs described by Rodrigues parameters can be gotten as

$$L_{AA'}{}^2 = (0)^2 + \left(\frac{\sqrt{3}L_m}{3\lambda_0^2}\left(1-2\Phi_1{}^2+2\Phi_2{}^2\right)-\frac{\sqrt{3}}{3}\eta L_m\right)^2 + \left(\frac{2\sqrt{3}L_m\Phi_1}{3\lambda_0^2}+z_{O'}\right)^2, \tag{40}$$

$$L_{BB'}{}^2 = \left(\frac{L_m}{\lambda_0^2}\left(\frac{\left(1+\Phi_1^2-\Phi_2^2\right)}{2}-\sqrt{3}\Phi_1\Phi_2\right)-\frac{\eta L_m}{2}\right)^2 + \left(\frac{L_m}{\lambda_0^2}\left(\Phi_1\Phi_2-\frac{\sqrt{3}\left(1+\Phi_1^2-\Phi_2^2\right)}{6}\right)+\frac{\sqrt{3}}{6}\eta L_m\right)^2 + \left(\frac{L_m}{\lambda_0^2}\left(-\Phi_2-\frac{\Phi_1}{\sqrt{3}}+\frac{z_O\lambda_0^2}{L_m}\right)\right)^2, \tag{41}$$

$$L_{CC'}{}^2 = \left(\frac{L_m}{\lambda_0^2}\left(\frac{-\left(1+\Phi_1^2-\Phi_2^2\right)}{2}-\sqrt{3}\Phi_1\Phi_2\right)+\frac{\eta L_m}{2}\right)^2 + \left(\frac{L_m}{\lambda_0^2}\left(-\Phi_1\Phi_2-\frac{\sqrt{3}\left(1+\Phi_1^2-\Phi_2^2\right)}{6}\right)+\frac{\sqrt{3}}{6}\eta L_m\right)^2 + \left(\frac{L_m}{\lambda_0^2}\left(\Phi_2-\frac{\Phi_1}{\sqrt{3}}+\frac{z_O\lambda_0^2}{L_m}\right)\right)^2. \tag{42}$$

The parallel manipulator includes three limbs denoted as AA', BB' and CC'. The following part shows the kinematic calculation of limb AA' firstly.
The coordinates of the connector A' can be expressed as

$$x_{A'} = 0\,, \tag{43}$$

$$y_{A'} = \frac{\sqrt{3}L_m}{3\lambda_0^2}\left(1-2\Phi_1^2+2\Phi_2^2\right), \tag{44}$$

$$z_{A'} = \frac{2\sqrt{3}L_m\Phi_1}{3\lambda_0^2}+z_{O'}\,. \tag{45}$$

Differentiating the above three equations with respect to time gets the sub-velocities of the connector A' as follows:

$$v_{A'x} = 0\,, \tag{46}$$

$$v_{A'y} = \frac{2L_m\left(-\Phi_1\left(3+4\Phi_2^2\right)\dot{\Phi}_1 + \Phi_2\left(1+4\Phi_1^2\right)\dot{\Phi}_2\right)}{\sqrt{3}\lambda_0^4}\,, \tag{47}$$

$$v_{A'z} = \frac{2L_m\left(\left(1-\Phi_1^2+\Phi_2^2\right)\dot{\Phi}_1 - 2\Phi_1\Phi_2\dot{\Phi}_2\right)}{\sqrt{3}\lambda_0^4} + \dot{z}\,. \tag{48}$$

The driving velocity of limb AA' obtained by differentiating its length with Rodrigues parameters can be shown as

$$\mathbf{v}_{AA'} = \frac{d\left(L_{AA'}\right)}{dt} = \frac{d\left(L_{AA'}^2\right)}{2L_{AA'}dt}\,. \tag{49}$$

According to the motion of limb AA' and the geometrical characteristics of this parallel manipulator, one can have

$$\mathbf{v}_{A'} = \mathbf{v}_{AA'}\mathbf{e}_{AA'} + \boldsymbol{\omega}_{AA'} \times \left(L_{AA'}\mathbf{e}_{AA'}\right)\,. \tag{50}$$

By dot-multiplying both sides of the above equation with $\mathbf{e}_{AA'} \times \left(L_{AA'}\mathbf{e}_{AA'}\right)$, Eq. (50) can be simplified as

$$\boldsymbol{\omega}_{AA'} = \mathbf{v}_{A'}\left(L_{AA'}\mathbf{e}_{AA'}\right)/L_{AA'}^2\,, \tag{51}$$

where $\mathbf{e}_{AA'}$ represents the unit vector of $\overline{AA'}$, and $\boldsymbol{\omega}_{AA'}$ is the angular velocity of limb AA'. Moreover, $\mathbf{v}_{A'} = \left[v_{A'x}\ \ v_{A'y}\ \ v_{A'z}\right]^T$.

Differentiating the velocities of the connector A' with respect to time gets the linear accelerations of this connector relative to the static coordinate system, three sub-accelerations of which along different axes of the static coordinate system can be written as

$$a_{A'x} = 0\,, \tag{52}$$

$$a_{A'y} = \frac{2L_m\left(-4\left(\Phi_1\dot{\Phi}_1+\Phi_2\dot{\Phi}_2\right)\left(-\Phi_1\left(3+4\Phi_2^2\right)\dot{\Phi}_1+\Phi_2\left(1+4\Phi_1^2\right)\dot{\Phi}_2\right)\right)}{\sqrt{3}\lambda_0^6} + \frac{2L_m\left(-\left(3+4\Phi_2^2\right)\dot{\Phi}_1^2+\left(1+4\Phi_1^2\right)\dot{\Phi}_2^2-\Phi_1\left(3+4\Phi_2^2\right)\ddot{\Phi}_1+\Phi_2\left(1+4\Phi_1^2\right)\ddot{\Phi}_2\right)}{\sqrt{3}\lambda_0^4}\,, \tag{53}$$

$$a_{A'z} = \frac{8L_m\left(\Phi_1\dot{\Phi}_1+\Phi_2\dot{\Phi}_2\right)\left(-\left(1-\Phi_1^2+\Phi_2^2\right)\dot{\Phi}_1+2\Phi_1\Phi_2\dot{\Phi}_2\right)}{\sqrt{3}\lambda_0^6} + \frac{2L_m\left(-2\Phi_1\left(\dot{\Phi}_1^2+\dot{\Phi}_2^2\right)+\left(1-\Phi_1^2+\Phi_2^2\right)\ddot{\Phi}_1-2\Phi_1\Phi_2\ddot{\Phi}_2\right)}{\sqrt{3}\lambda_0^4} + \ddot{z}\,. \tag{54}$$

The angular acceleration can be obtained by differentiating the angular velocity of limb AA' with respect to time as follows:

$$\zeta_{AA'} = \left(a_{AA'}\left(L_{AA'}^2\right) - \mathbf{v}_{AA'}\left(L_{AA'}^2\right)'\right)\left(L_{AA'}\mathbf{e}_{AA'}\right)\Big/L_{AA'}^4\,. \tag{55}$$

Similarly, the velocities and the accelerations of the other limbs can also be gotten by the corresponding calculations.

4. Forward Kinematic Analysis of 3-UCR Parallel Robot Leg

The forward position-stance analysis of the parallel manipulators is the basis of structure synthesis, kinematic analysis and dynamic optimization, and many researchers had paid more attention to it gradually (Ruggiu, 2008; Kim & Park, 2001; Jaime et al., 2006; Lu et al., 2008). However, the forward position-stance analysis of the parallel manipulator is more difficult than the inverse position-stance analysis because it is essential to solve the multivariate nonlinear equations.

4.1 Analytical model

The constraint equations of the parallel robot leg can be obtained by the geometrical characteristics, and the variables in the equations can be eliminated by the successive elimination method. Then the constraint equations are changed into the unary polynomial equation.

Three joints, denoted as A', B', and C', can be described by another method by the angle between driving limbs and moving platform. The above angles are assumed as a_A, a_B, and a_C respectively. And the joints in the moving platform can be expressed as

$$\left(x_{A'}, y_{A'}, z_{A'}\right) = \left(0, \frac{\sqrt{3}}{3}L_m - L_{AA'}\cos\left(\alpha_A\right), L_{AA'}\sin\left(\alpha_A\right)\right), \tag{56}$$

$$\left(x_{B'}, y_{B'}, z_{B'}\right) = \left(-\frac{1}{2}L_m + \frac{\sqrt{3}}{2}L_{BB'}\cos\left(\alpha_B\right), -\frac{\sqrt{3}}{6}L_m + \frac{1}{2}L_{BB'}\cos\left(\alpha_B\right), L_{BB'}\sin\left(\alpha_B\right)\right), \tag{57}$$

$$\left(x_{C'}, y_{C'}, z_{C'}\right) = \left(\frac{1}{2}L_m - \frac{\sqrt{3}}{2}L_{CC'}\cos\left(\alpha_C\right), -\frac{\sqrt{3}}{6}L_m + \frac{1}{2}L_{CC'}\cos\left(\alpha_C\right), L_{CC'}\sin\left(\alpha_C\right)\right). \tag{58}$$

Three joints in the moving platform are symmetrical and the distances between two joints of them are denoted as L_m. So the equations can be gotten as follows:

$$\left(x_{B'} - x_{A'}\right)^2 + \left(y_{B'} - y_{A'}\right)^2 + \left(z_{B'} - z_{A'}\right)^2 = {L_m}^2, \tag{59}$$

$$\left(x_{C'} - x_{A'}\right)^2 + \left(y_{C'} - y_{A'}\right)^2 + \left(z_{C'} - z_{A'}\right)^2 = {L_m}^2, \tag{60}$$

$$\left(x_{C'} - x_{B'}\right)^2 + \left(y_{C'} - y_{B'}\right)^2 + \left(z_{C'} - z_{B'}\right)^2 = {L_m}^2. \tag{61}$$

Substituting the coordinates of three joints into the above equation gives

$${L_{AA'}}^2 + L_{BB'}\left(-\sqrt{3}L_m\cos\left(\alpha_B\right) + L_{BB'}\right) + L_{AA'}\left(-\sqrt{3}L_m\cos\left(\alpha_A\right) + \left(\cos\left(\alpha_A\right)\cos\left(\alpha_B\right) - 2\sin\left(\alpha_A\right)\sin\left(\alpha_B\right)\right)L_{BB'}\right) = 0, \tag{62}$$

$${L_{AA'}}^2 + L_{CC'}\left(-\sqrt{3}L_m\cos\left(\alpha_C\right) + L_{CC'}\right) + L_{AA'}\left(-\sqrt{3}L_m\cos\left(\alpha_A\right) + \left(\cos\left(\alpha_A\right)\cos\left(\alpha_C\right) - 2\sin\left(\alpha_A\right)\sin\left(\alpha_C\right)\right)L_{CC'}\right) = 0, \tag{63}$$

$${L_{BB'}}^2 + L_{CC'}\left(-\sqrt{3}L_m\cos\left(\alpha_C\right) + L_{CC'}\right) + L_{BB'}\left(-\sqrt{3}L_m\cos\left(\alpha_B\right) + \left(\cos\left(\alpha_B\right)\cos\left(\alpha_C\right) - 2\sin\left(\alpha_B\right)\sin\left(\alpha_C\right)\right)L_{CC'}\right) = 0. \tag{64}$$

Substituting the universal trigonometric functions into the above transcendental equations and supposing $\sin(\alpha_i) = 2x_i/(1+x_i^2)$, $\cos(\alpha_i) = (1-x_i^2)/(1+x_i^2)$ where $x_i = \tan(\alpha_i/2)$ (i=A, B, C), can simplify the above equations as follows:

$$G_1 x_2^2 + H_1 x_2 + J_1 = 0\,, \tag{65}$$

$$G_2 x_3^2 + H_2 x_3 + J_2 = 0\,, \tag{66}$$

$$G_3 x_3^2 + H_3 x_3 + J_3 = 0\,, \tag{67}$$

where $G_1 = -\sqrt{3}L_m L_{AA'} + L_{AA'}^2 + \sqrt{3}L_m L_{BB'} - L_{AA'}L_{BB'} + L_{BB'}^2 + \sqrt{3}L_m L_{AA'}x_1^2 + L_{AA'}^2 x_1^2 + \sqrt{3}L_m L_{BB'}x_1^2 + L_{AA'}L_{BB'}x_1^2 + L_{BB'}^2 x_1^2$,

$G_2 = -\sqrt{3}L_m L_{AA'} + L_{AA'}^2 + \sqrt{3}L_m L_{CC'} - L_{AA'}L_{CC'} + L_{CC'}^2 + \sqrt{3}L_m L_{AA'}x_1^2 + L_{AA'}^2 x_1^2 + \sqrt{3}L_m L_{CC'}x_1^2 + L_{AA'}L_{CC'}x_1^2 + L_{CC'}^2 x_1^2$,

$G_3 = -\sqrt{3}L_m L_{BB'} + L_{BB'}^2 + \sqrt{3}L_m L_{CC'} - L_{BB'}L_{CC'} + L_{CC'}^2 + \sqrt{3}L_m L_{BB'}x_2^2 + L_{BB'}^2 x_2^2 + \sqrt{3}L_m L_{CC'}x_2^2 + L_{BB'}L_{CC'}x_2^2 + L_{CC'}^2 x_2^2$,

$J_1 = -\sqrt{3}L_m L_{AA'} + L_{AA'}^2 - \sqrt{3}L_m L_{BB'} + L_{AA'}L_{BB'} + L_{BB'}^2 + \sqrt{3}L_m L_{AA'}x_1^2 + L_{AA'}^2 x_1^2 - \sqrt{3}L_m L_{BB'}x_1^2 - L_{AA'}L_{BB'}x_1^2 + L_{BB'}^2 x_1^2$,

$J_2 = -\sqrt{3}L_m L_{AA'} + L_{AA'}^2 - \sqrt{3}L_m L_{CC'} + L_{AA'}L_{CC'} + L_{CC'}^2 + \sqrt{3}L_m L_{AA'}x_1^2 + L_{AA'}^2 x_1^2 - \sqrt{3}L_m L_{CC'}x_1^2 - L_{AA'}L_{CC'}x_1^2 + L_{CC'}^2 x_1^2$,

$J_3 = -\sqrt{3}L_m L_{BB'} + L_{BB'}^2 - \sqrt{3}L_m L_{CC'} + L_{BB'}L_{CC'} + L_{CC'}^2 + \sqrt{3}L_m L_{BB'}x_2^2 + L_{BB'}^2 x_2^2 - \sqrt{3}L_m L_{CC'}x_2^2 - L_{BB'}L_{CC'}x_2^2 + L_{CC'}^2 x_2^2$,

$H_1 = -2L_{AA'}L_{BB'}x_1$, $H_2 = -2L_{AA'}L_{CC'}x_1$, $H_3 = -2L_{BB'}L_{CC'}x_2$.

The above equations can be simplified into the polynomial with sixteen degrees having one variable, and the main process can be described as the following steps.
At first, simplifying the two equations about x_3 gives

$$\begin{bmatrix} G_2H_3 - G_3H_2 & G_2J_3 - J_2G_3 \\ J_2G_3 - G_2J_3 & J_2H_3 - H_2J_3 \end{bmatrix} \begin{bmatrix} x_3 \\ 1 \end{bmatrix} = \begin{bmatrix} 0 \\ 0 \end{bmatrix}. \tag{68}$$

By analyzing the geometrical characteristics of the parallel robot leg, it is obvious that $x_3 \neq 0$. So the following equation can be gotten as

$$(G_2H_3 - G_3H_2)(J_2H_3 - H_2J_3) - (G_2J_3 - J_2G_3)^2 = 0\,. \tag{69}$$

Then simplifying x_2 in the above equation gives

$$Q_4 x_2^4 + Q_3 x_2^3 + Q_2 x_2^2 + Q_1 x_2 + Q_0 = 0\,, \tag{70}$$

where Q_i (i=0, 1, 2, 3, 4) is the polynomial about x_1 having not more than four degrees. Because of $G_1 x_2^2 + H_1 x_2 + J_1 = 0$, combining the above two equations can get the following equation as

$$\begin{bmatrix} H_1Q_4 - G_1Q_3 & J_1Q_4 - G_1Q_2 & -G_1Q_1 & -G_1Q_0 \\ G_1Q_2 - J_1Q_4 & G_1Q_1 + H_1Q_2 - J_1Q_3 & G_1Q_0 + H_1Q_1 & H_1Q_0 \\ G_1 & H_1 & J_1 & 0 \\ 0 & G_1 & H_1 & J_1 \end{bmatrix} = 0 . \tag{71}$$

The above equation is the polynomial about x_1 having sixteen degrees, and the corresponding solutions have sixteen groups. Putting the angle values of a_i (i=1, 2, 3) into the coordinates joints in the moving platform gives the forward position-stance solutions of three spheral joints. Because three spheral joint coordinates do not exist in the same line, the plane decided by the spheral joints can be solved. Moreover, the coordinates of any points in the moving platform can also be gotten. So knowing the exact values of the inputs, denoted as $L_{AA'}$, $L_{BB'}$, $L_{CC'}$, can get the corresponding values of the outputs, denoted as Φ_1, Φ_2, $Z_{O'}$. And the forward position-stance model of the parallel robot leg with the analytical form has been established.

4.2 Numerical model

Though all position-stance solutions of the robot leg can be gotten by the analytical model, the elimination process is complicated and sometimes it is not necessary to get all of them in practice. In the given workspace, the only one forward position-stance solution of the structure is available. So the numerical solutions can be easier to be calculated and it becomes the feasible method to analyze the forward kinematics.

4.2.1 Iterative algorithm

Bracketing methods such as the bisection method and the false position method of finding roots of a nonlinear equation require bracketing of the root by two guesses. These methods are always convergent since they are based on reducing the interval between the two guesses to zero on the root. In the Newton-Raphson method, only one initial guess of the root is needed to get the iterative process started to find the root of an equation. This method is based on the principle that if the initial guess of the root of f(x)=0 is at x_i , then if one draws the tangent to the curve at f(x_i), the point x_{i+1} where the tangent crosses the x-axis is an improved estimate of the root. So the Newton-Raphson method is applied as the iterative algorithm.

The iterative steps of numerical model of the parallel robot leg can be written as follows.

At first, the iterative function is defined as

$$\mathrm{g}\left(\Phi_1,\Phi_2,Z_{O'}\right) = \mathbf{L}_{II'}\left(\Phi_1,\Phi_2,Z_{O'}\right) - \mathbf{L}_{II'M} , \tag{72}$$

where $\mathbf{L}_{II'}\left(\Phi_1,\Phi_2,Z_{O'}\right) = \left[AA'\left(\Phi_1,\Phi_2,Z_{O'}\right)\ BB'\left(\Phi_1,\Phi_2,Z_{O'}\right)\ CC'\left(\Phi_1,\Phi_2,Z_{O'}\right)\right]^T$ and $\mathbf{L}_{II'M}$ is the measured values of three driving limbs. Substituting the iterated values of three outputs into the inverse kinematic model of the parallel robot leg can obtain the theoretical values of three driving limbs.

Based on the Newton-Raphson method, supposing Q_K as $\left(\Phi_{1K},\Phi_{2K},Z_{O'K}\right)$ gets the following equation as

$$Q_{K+1} = Q_K - \frac{g(Q_K)}{g'(Q_K)}, \tag{73}$$

where $g'(Q_K)$ can be replaced by the Jacobi matrix of the robot leg. That can be expressed as

$$Q_{K+1} = Q_K - \frac{\left(\mathbf{L}_{II'}(\Phi_1, \Phi_2, Z_{O'}) - \mathbf{L}_{II'M}\right)}{J_E}. \tag{74}$$

The tolerances of the driving limbs are defined as $\mathbf{L}_{II'\square}$. If the iterative terminational condition could be reached, the corresponding outputs about Q_{K+1} can be calculated by the above equation. Corresponding to the preceding inputs, the values of three outputs are the forward kinematic solutions of 3-UCR parallel robot leg.

4.2.2 Numerical simulation

In order to validate the iterative process of forward kinematics, the initial structure parameters of 3-UCR parallel robot leg need to be defined and put into the Matlab program written by the preceding steps. Then the output values of 3-UCR parallel robot leg can be obtained after several iterative circles.

Firstly, the distances between the joints in the moving platform, denoted as L_m, are initialized as $50\sqrt{3}$ mm, and the circumcircle radius of the equilateral triangle formed by three spheral joints is set as 50mm. The distances between the rotational joints, denoted as L_B, are $68\sqrt{3}$ mm, and the corresponding circumcircle radius of the equilateral triangle is 68mm.

For the purpose of getting the target values of the outputs, it is necessary to assume the position-stance outputs as $[\Phi_1 \Phi_2 z_{O'}]$ = [-0.2 0.5 320] in advance. By the relations among three spheral joints and the outputs, the position-stance output values caused by the other related DOF can be obtained as $[\Phi_3 x_{O'} y_{O'}]$ = [0 7.7519 8.1395].

Substituting the output values into the inverse kinematic model gives $[L_{AA'} L_{BB'} L_{CC'}]$ = [304.7719 295.1586 364.8734]. The units in the above matrix are millimeter, and the above input values of three driving limbs are assumed as the measured values by the displacement sensors.

The choice of the initial values in the course of calculation is important, especially the parallel manipulators, because the number of the forward position-stance solutions of the parallel manipulators is more than the number of the serial manipulators. If the errors of initial values are enough large, the other group of forward solutions would be gotten. So the initial search values of the outputs are set as Q_0 = [-0.22 0.48 318]^T.

By calculating circularly the iterative parameter, denoted as $\{Q_K\}_{K=0}^{\infty}$, and defining the terminational tolerance value as $\mathbf{L}_{II'\square}$=0.0001, the accurate values of the outputs can be obtained when the calculated tolerance is less than the terminational tolerance. According to the above parameter choice, the output values in the different iterative steps have been solved and the corresponding values are written in Table 1.

	Φ_1	Φ_2	$z_{O'}$
0	-0.22	0.48	318
1	-0.196089	0.505499	320.46100
2	-0.200635	0.499836	319.90179
3	-0.199858	0.499836	320.01285
4	-0.200032	0.499996	319.99716
5	-0.199993	0.500000	320.00063
6	-0.200002	0.500000	319.99992

Table 1. Numerical solution of the outputs parameters of forward kinematics

The data in Table 1 have been calculated by the taking or rejecting way, and the values of the last two iterative steps meet with the iterative terminational condition. Calculation of the six cycles shows that the Newton-Raphson method can search the exact forward position-stance solutions rapidly. However, for the reason of the choice of initializations and limitation of iteration step, it is necessary to pay attention to solution precision and algorithm stability. So we need take the following measures during the calculation process of forward kinematics.

At first, if the function equals to zero, the program would have faults. So we need to judge the value of $f'(Q)$ and eliminate the condition. Then the slope value of $f'(Q)$ is so little that $\{Q_K\}$ converges to another group of the solutions. So we should define the initial values accurately. Finally, if the items of $\{Q_K\}$ tend to repetition, the calculation process would run into limitless cycles. So the maximum steps should be chosen to improve the validity of the program.

5. Conclusions

Based on principal screw theory and imaginary manipulator method, the kinematic characteristics of 3-UCR spatial parallel robot leg with three DOF were analyzed. According to the topologic structure of limbs, the screw coordinate system was obtained and the kinematics of limbs was studied. By the relation of the matrices of influence coefficient between limbs and moving platform, the kinematic model with the screw coordinates was established. It shows that the matrices of influence coefficient is only dependent on the inputs and kinematic parameters and the method analyzing instantaneous motion is fit for others kinds of lower-mobility parallel manipulators. The instantaneous pitches of the principal screws gained decide that the kind of manipulator has always three DOF including one translation and two rotations. By the numerical simulation when the moving platform is parallel to the base, the pitch analysis of principal screws validates the kinematic characters of 3-UCR parallel robot leg.

A new method to describe the position-stance of 3-UCR parallel robot leg was proposed based on the Rodrigues theory. Comparing with others methods, the kinematic model with Rodrigues parameters has the advantages including least computational parameters, no trigonometric function calculation and convenient real-time control. The model of the inverse kinematics was established and the inverse solutions of the position-stance were obtained by analyzing the topologic structure of 3-UCR parallel robot leg. By analyzing the vectors of the manipulator, the velocity and acceleration models of moving platform, limbs

and end-effector were deduced. According to the designed kinematic track, it is convenient to control accurately 3-UCR parallel robot leg by the inverse kinematic model.
According to the topologic system of 3-UCR parallel robot leg, the geometrical constraints are obtained. And the forward kinematic model with analytical expressions can be established by eliminating the unknown terms. It is shown that the analytical solutions of the forward kinematic model have 16 groups. In order to decrease the number of solutions and get the exact position-stance of 3-UCR parallel robot leg, the Newton-Raphson method was used to search the best numerical solutions by the judgment of the terminal value. The corresponding numerical simulation proved that the exact forward solution can be found rapidly by the iterative steps. Moreover, aiming at improving the numerical precision, some measures on the choice of initial value and iterative step had been put forward. The forward kinematic model provides the basis of the perfect control of 3-UCR parallel robot leg.

6. Acknowledgment

Financial support for this work, provided by the National Natural Science Foundation of China (Grant No. 50905180, 60808017) and the youth foundation and Qihang Project of China University of Mining and Technology, are gratefully acknowledged.

7. References

Alon, W. & Moshe, S. (2006). Screw theory tools for the synthesis of the geometry of a parallel robot for a given instantaneous task. *Mechanism and Machine Theory*, 41: 656-670.

Altmann, S. L. (1986). *Rotations, quaternions, and double groups*, Clarendon Press, Oxford, England.

Baker, C.; Morris, A. & Ferguson, D. (2004). A campaign in autonomous mine mapping, *IEEE International Conference on Robotics and Automation*, New Orleans, pp. 2004-2009.

Ball, R. S. (1900). *A treatise on the theory of screws* . Cambridge University Press, Cambridge.

Carretero, J. A.; Podhorodeski, R. P. & Nahon, M. A. ; et al. (2000). Kinematic analysis and optimization of a new three degree-of-freedom spatial parallel manipulator, *Journal of Mechanical Design*, 122(1): 17-24.

Cayley, A. (1875). On three-bar motion, *Proceedings of the London Mathematical Society V II*, pp. 136-166.

Clavel R. (1988). DELTA, A Fast Robot with Parallel Geometry. *The 18th International Symposium on Industrial Robot*, Lausanne, pp. 91-100.

Dai, J. (2006). An historical review of the theoretical development of rigid body displacements from Rodrigues parameters to the finite twist. *Mechanism and Machine Theory*, 41: 41-52.

Dunlop, G. R. & Jones, T. P. (1997). Position analysis of a 3-DOF parallel manipulator, *Mechanism and Machine Theory*, 32(8): 903-920.

Fang, Y. F. & Huang Z. (1998). Analytical identification of the principal screws of the third order screw system. *Mechanism and Machine Theory*, 33(7): 987-992.

Fang, Y. F. & Tsai, L. W. (2004). Structure synthesis of a class of 3-DOF rotational parallel manipulators. *IEEE Transactions on Robotics and Automation*, 1: 117-121.

Gabmann, B.; Zacharias, F. & Zollner, J. (2005). Location of walking robots, *IEEE International Conference on Robotics and Automation*, Barcelona, Spain, pp. 1471-1476.

Hunt, K. H. (1978). *Kinematic geometry of mechanisms*. Cambridge University Press, Cambridge.

Jaime, G. A.; Jose, M. R. & Gursel, A. (2006). Kinematics and singularity analysis of a 4-dof parallel manipulator using screw theory. *Mechanism and Machine Theory*, 41: 1048-1061.

Kim, J. (2001). Design and analysis of an overactuated parallel mechanism for rapid machining, *IEEE Trans. Robotics & Automation*, 17(4): 423-434.

Kim, J. & Park, F. (2001). Direct kinematic analysis of 3-RS parallel mechanisms. *Mechanism and Machine theory*, 36: 1121-1134.

Kindermann, H. & Cruse, H. (2002). MMC – a new numerical approach to the kinematics of complex manipulators. *Mechanism and Machine Theory*, 37: 375-394.

Koditschek, D.; Full, R. & Buehler, M. (2004). Mechanical aspects of legged locomotion control, *Arthropod Structure & Development*, 33: 251-272.

Lu, Y.; Shi, Y. & Hu, B. (2008). Kinematic analysis of two novel 3UPU Ⅰ and 3UPU Ⅱ PKMs. *Robotics and Autonomous Systems*, 56: 296-305.

Pouliot, N. A.; Nahon, M. A. & Gosselin, C. M. (1996). Analysis and comparison of the motion simulation capabilities of three degree-of-freedom flight simulators, *Proceedings of AIAA Flight Simulation Technologies Conference*, San Diego, PP. 37-47.

Ruggiu, M. (2008). Kinematics analysis of the CUR translational manipulator. *Mechanism and Machine Theory*, 43: 1087-1098.

Santos, P.; Estremera, J. & Garcia, E. (2005). Including joint torques and power consumption in the stability margin of walking robots, *Autonomous Robots*, 18: 43-57.

Sokolov, A. & Xirouchakis, P. (2005). Kinematics of a 3-DOF parallel manipulator with an R-P-S joint structure. *Robotica*, 23: 207-217.

Sokolov, A. & Xirouchakis, P. (2006). Singularity analysis of a 3-DOF parallel manipulator with R-P-S joint structure. *Robotica*, 24: 131-142.

Tanaka, J.; Suzumori, K. & Takata, M. (2005). A mobile Jack robot for rescue operation, *IEEE International Workshop on Safety, Security and Rescue Robotics*, Kobe Japan, pp. 99-104.

Wang, W.; Du, Z. & Sun, L. (2007). Obstacle performance analysis of mine research robot based on terramechanics, *IEEE International Conference on Mechatronics and Automation*, Harbin, China, pp. 1382-1387.

Wang, Y. & Wang, Y. (2005). Inverse kinematics of variable geometry parallel manipulator. *Mechanism and Machine Theory*, 40: 141-155.

Robot Manipulators New Achievements

Edited by Aleksandar Lazinica and Hiroyuki Kawai

ISBN 978-953-307-090-2
Hard cover, 718 pages
Publisher InTech
Published online 01, April, 2010
Published in print edition April, 2010

Robot manipulators are developing more in the direction of industrial robots than of human workers. Recently, the applications of robot manipulators are spreading their focus, for example Da Vinci as a medical robot, ASIMO as a humanoid robot and so on. There are many research topics within the field of robot manipulators, e.g. motion planning, cooperation with a human, and fusion with external sensors like vision, haptic and force, etc. Moreover, these include both technical problems in the industry and theoretical problems in the academic fields. This book is a collection of papers presenting the latest research issues from around the world.

InTech Europe
University Campus STeP Ri
Slavka Krautzeka 83/A
51000 Rijeka, Croatia
Phone: +385 (51) 770 447
Fax: +385 (51) 686 166
www.intechopen.com

InTech China
Unit 405, Office Block, Hotel Equatorial Shanghai
No.65, Yan An Road (West), Shanghai, 200040, China
中国上海市延安西路65号上海国际贵都大饭店办公楼405单元
Phone: +86-21-62489820
Fax: +86-21-62489821

IntechOpen